AIP Advances

The pore-load modulus of ordered nanoporous materials with surface effects

Mingchao Liu, Jian Wu, Yixiang Gan, and C. Q. Chen

Citation: AIP Advances **6**, 035324 (2016); doi: 10.1063/1.4945441
View online: http://dx.doi.org/10.1063/1.4945441
View Table of Contents: http://scitation.aip.org/content/aip/journal/adva/6/3?ver=pdfcov
Published by the AIP Publishing

The pore-load modulus of ordered nanoporous materials with surface effects

Mingchao Liu,[1] Jian Wu,[1] Yixiang Gan,[2] and C. Q. Chen[1,a]
[1]*Department of Engineering Mechanics and Center for Nano and Micro Mechanics, AML, Tsinghua University, Beijing 100084, China*
[2]*School of Civil Engineering, The University of Sydney, Sydney, NSW 2006, Australia*

(Received 23 January 2016; accepted 23 March 2016; published online 31 March 2016)

Gas and liquid adsorption-induced deformation of ordered porous materials is an important physical phenomenon with a wide range of applications. In general, the deformation can be characterized by the pore-load modulus and, when the pore size reduces to nanoscale, it is affected by surface effects and shows prominent size-dependent features. In this Letter, the influence of surface effects on the elastic properties of ordered nanoporous materials with internal pressure is accounted for in a single pore model. A porosity and surface elastic constants dependent closed form solution for the size dependent pore-load modulus is obtained and verified by finite element simulations and available experimental results. In addition, it is found to depend on the geometrical arrangement of pores. This study provides an efficient tool to analyze the surface effects on the elastic response of ordered nanoporous materials. [http://dx.doi.org/10.1063/1.4945441]

Ordered porous materials have attracted increasing attention in recent years due to their unique optical, electrical, and catalytic properties.[1–4] With the development of fabrication technology, the pore morphologies and porosities can be accurately controlled by electrochemical etching, depending on the doping and etching conditions.[5] Understanding of the relationship between their structures and mechanical properties is necessary for their functional applications.[3,4] The major focus of most previous works has been limited to the elastic response of porous samples to external mechanical loads and the related properties including the effective bulk and Young's moduli.[6–8] However, the elastic response of porous materials to internal pressure loadings has attracted much less attention.[9]

There are numerous application examples of porous materials, especially for pores in nanoscale subjecting to internal loading, such as gas or fluid adsorption in nanoporous solids in the fields of geology, biology, chemistry, etc.[4,10] Such nanoporous solids usually have ordered channel-like independent cylinder pores. In the process of adsorption or desorption of gas or fluid, as a consequence of the physical and chemical interactions between the guest molecules and the solid pore walls, the solid walls either contract or expand.[11,12] Such phenomena are known as adsorption-induced deformation.[13–18] Since the expansion of charcoal upon adsorption of CO_2 and other gases was reported in the 1920s,[13,14] adsorption-induced deformation has been observed for various porous systems, e.g., porous silicon,[15] zeolites,[16] aerogels,[17] and low-k films.[18] Due to the potential applications to design sensors and actuators,[19,20] the issue of adsorption-induced deformation received renewed attention in recent years.[21,22] The newly- developed experimental techniques, such as in situ small-angle X-ray and neutron diffractometry, provided powerful tools to quantitatively investigate these nanoporous systems.[23]

Based on the experimental methods, adsorption deformation was measured for highly ordered two dimensional (2D) pore lattice structures, such as MCM-41 or SBA-15.[21–24] The adsorption-induced strain was caused by capillary pressure which acts as a radial stress on the pore walls.The

[a]Corresponding author. Tel/Fax: +86 10 62783488; Email: chencq@tsinghua.edu.cn (C.Q. Chen)

ratio between the pressure in the pore and the experimentally measured strain can be defined as the pore-load modulus which can be expressed as a function of porosity and the elastic constants of the solid skeleton.[21] Different from bulk and Young's moduli, the pore load modulus is a metrics of the deformability of the sample under the internal loading, e.g., the pressure inside the pore.

There are several theoretical models proposed to describe the relationship between the pore-load modulus and the geometric and material constants.[21,22,24–27] In the early attempt given by Dolino *et al.*,[25] an analytical expression for the pore-load modulus was derived as a function of material parameters. Prass *et al.*[21] proposed another model based on the similarity of the adsorption-induced strain and the hoop stress in the thin-walled cylinders. Recently, a more accurate theoretical model was given by Gor *et al.*,[27] in which a single cylindrical pore was taken as a unit cell and elastic solution for the pressurized thick-walled cylinders was adopted to calculate the engineering strain in the unit cell. One important hypothesis in the model is that the axisymmetric conditions used implies the stress vanish at half of the distance between neighboring pores. The analytical model is found to match the FEM results well and only slightly overestimate the corresponding FEM results.

Classical theory of elasticity, used in the aforementioned models, does not admit intrinsic size dependency in the elastic solutions. At nano-scale, however, the surface energy of structures plays a significant role in their mechanical properties.[28–30] Similarly, when the pore size reduces to nano-scale, the high surface area to volume ratio of the ordered nanoporous materials introduces notable surface effects into their mechanical properties of the materials,[31–34] while all previous models did not consider the surface effect on the adsorption-induced deformation.

In this Letter, a theoretical framework considering the surface effect on the pore-load modulus of ordered nanoporous materials is developed, in which a micromechanical model based on the elastic solution of a single-pore model (i.e., a thick-wall cylinder) is adopted to take the pressure on the outer radius into account. The influence of the geometrical arrangement of pores is also considered and the influence of the surface energy on the adsorption-induced deformation is included by introducing surface elastic constants. The proposed model can be used to calculate the pore load modulus and reflect the size effect at nanoscale. When the surface effect is negligible, the theoretical model reduces to the classical solution without the size effect. In order to validate the proposed analytical model, the pore-load modulus of a parallel cylindrical pores distributed on two lattices, i.e., triangular (also known as the hexagonal) and square lattices, have been calculated numerically using FEM. The predictions of our analytical model show a good agreement with the FEM results. Finally, the influence of surface energy on the adsorption-induced deformation and size-dependent pore load modulus are discussed.

Note that the surface to volume ratio in nanoporous materials is huge. The influence of surface energy on their mechanical performance becomes important and should be taken into account. Generally, the influence of surfaces can be described either by surface energy or surface stress. For a linear isotropic surface without residual surface tension, the surface stress $\sigma^s_{\alpha\beta}$ is given by[28,35]

$$\sigma^s_{\alpha\beta} = 2\mu_s\varepsilon^s_{\alpha\beta} + \lambda_s\varepsilon_{rr}\delta_{\alpha\beta}, \tag{1}$$

where μ_s and λ_s are the surface Lame constants (in the unit of N/m), which can be determined through atomic simulations or experiments.[36] On the interface, the equilibrium equations and the constitutive relations on the surface are expressed as $\sigma_{ij}n_in_j = \sigma^s_{\alpha\beta}\kappa_{\alpha\beta}$, where n_i is the normal vector of the surface, and $\kappa_{\alpha\beta}$ is the curvature of the surface. For a curved surface, such as a circular hole, the surface stress and the surface curvature play a dominant role in the surface equilibrium conditions.

For typical ordered nanoporous materials like MCM-41 or SBA-15, as illustrated in Fig. 1(a), all exhibiting cylindrical pores are arranged on a well ordered 2D triangular lattice. Considering the thickness of the plate is much larger than the pore diameter size, the porous plate can be regards as under plane strain condition. Gor *et al.* pointed out that the dilatational strain in the plate with many pores can be approximated to the engineering strain of the unit cell of pressurized cylinder, with the outer diameter equaling half of the pore spacing.[27] However, it should also be noted that each cylinder will be affected by the neighboring cylinders. For nanoporous materials with triangular lattice,

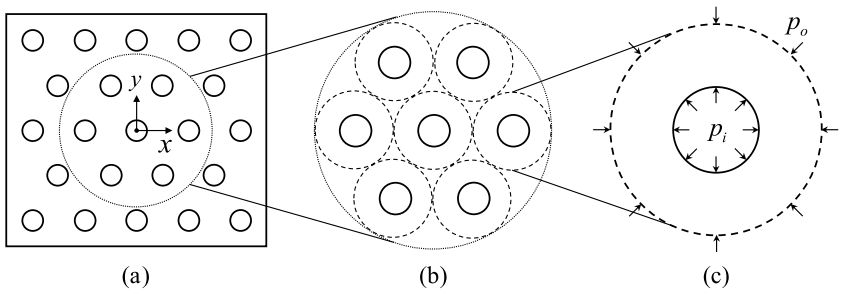

FIG. 1. (a) Schematic of a two-dimensional ordered porous material consisting of parallel cylindrical pores distributed on a triangular lattice; (b) The interaction between the neighboring pores for the thick-wall cylinder unit cell; (c) The unit cell of thick-wall cylinder with boundary conditions.

there are six pores near the central unit cell. (See Fig. 1(b), the enlarged sub-graph in Fig. 1(a)). Hence, the outer boundary of the cylinder cannot be considered as free surface.

Let us consider a single pressurized thick-wall cylinder with inner radius a and outer radius b, subjecting the inner and outer pressure p_i and p_o under the plane-strain condition, as shown in Fig. 1(c). According to the classical theory of elasticity,[37] the stress components in the bulk can be express as

$$\sigma_{rr} = 2C + \frac{A}{r^2},\ \sigma_{\theta\theta} = 2C - \frac{A}{r^2}, \tag{2}$$

and the radial displacement is

$$u(r) = \frac{1+v}{E}\left[2(1-2v)Cr - \frac{A}{r}\right], \tag{3}$$

where E and v are the Young's modulus and Poisson ratio of the solid matrix, respectively, and A and C are unknown constants to be determined by boundary conditions.

According to the constitutive relation for the bulk material, the hoop strain on the inner surface of the cylinder is related to the bulk stresses by

$$\varepsilon_{\theta\theta} = \frac{1-v^2}{E}\left(\sigma_{\theta\theta} - \frac{v}{1-v}\sigma_{rr}\right). \tag{4}$$

Thus, the surface stress $\sigma^s_{\theta\theta}$ at $r = a$, as given by Eq. (1), can be obtained as

$$\sigma^s_{\theta\theta} = (2\mu_S + \lambda_S)\,\varepsilon_{\theta\theta}. \tag{5}$$

Since the cylinder unit cell is extracted from the nanoporous plate, the outer surface is not exposed as a free surface. Thus the surface energy only affects the inner surface of the cylinder. Considering this added effect from the surface stress, the boundary conditions are given as

$$\sigma_{rr}|_{r=a} = -p_i + \frac{\sigma^s_{\theta\theta}}{a},\ \sigma_{rr}|_{r=b} = -p_o. \tag{6}$$

Substitution of Eqs. (2) and (6) into Eq. (6) yields

$$\begin{cases} A = \dfrac{a^2b^2\{[1-(1+v)(1-2v)k]p_o - p_i\}}{[1+(1+v)k]b^2 - [1-(1+v)(1-2v)k]a^2} \\ C = \dfrac{1}{2}\dfrac{a^2p_i - b^2[1+(1+v)k]p_o}{[1+(1+v)k]b^2 - [1-(1+v)(1-2v)k]a^2} \end{cases}, \tag{7}$$

where $k = (2\mu_S + \lambda_S)/(Ea)$ is a dimensionless parameter describing the relative contribution of surface effect. For a given nanoporous material, k increases as the pore radius decreases. When the pore size is large enough so that k is negligible, Eq. (7) can reduce to the classical elastic results of the pressurized thick-wall cylinder.[37]

It can be found that the inner pressure p_i is the pressure that the fluid exerts on each pore wall, and the outer pressure p_o was induced by the interaction between the neighboring pores. Note that, by introducing the non-zero outer pressure p_o, the effects of different geometrical configurations can be considered. If we consider an infinite plate containing a single pore, subjected to the uniform pressure p_i at the radial direction of the pore, the radial stress is $\sigma_r = (a^2/r^2)p_i$. The interaction induced pressure at the outer radius of the cylinder can be assumed to be

$$p_o = \alpha \cdot \sigma_r|_{r=b} = \alpha\left(\frac{a}{b}\right)^2 p_i, \tag{8}$$

where α is a factor depending on the geometrical arrangement of pores. For nanoporous materials with the triangular lattice arrangement, there are six pores near the central unit cell (see Fig. 1(b)), and considering the interaction of the adjacent two pores at the same time, the factor should be choose as 2/6 (i.e., $\alpha = 1/3$). Similarly, the factor for the square lattice arrangement is 2/4 ($\alpha = 1/2$).

The radial displacement can be completely determined by substituting Eqs. (7) and (8) into Eq. (3). And the engineering strain of a single cylinder pore can be calculated as $\varepsilon_e = u(b)/b$. Thus, the pore-load modulus of the nanoporous material can be then obtained by the definition $M_{pl} = p_i/\varepsilon_e$ as

$$M_{pl} = \frac{E\{[1+(1+v)k]-[1-(1+v)(1-2v)k]\xi\}}{(1+v)\{(1-2v)[1-\alpha(1+(1+v)k)]-[\alpha(1-(1+v)(1-2v)k)\xi-1]\}\xi}, \tag{9}$$

where $\xi = a^2/b^2$ is the porosity factor which is related to porosity φ by $\xi = \pi/2\sqrt{3}\cdot\varphi$ for the triangular lattice and $\xi = \pi/4\cdot\varphi$ for the square lattice. For a porous material under plane stress condition, the parameters E and v should be replaced by $E/(1-v^2)$ and $v/(1-v)$, respectively.

It can be found that the pore-load modulus depends on the material properties E, v, porosity φ, and the geometrical arrangement factor α. Moreover, the surface effect parameter k plays an important role on the pore-load modulus of nanoporous material. As we have mentioned before, k is the parameter describing the relative contribution of surface effect. For the porous material with given mechanical properties, k is increasing with the decreasing of the pore radius, and indicating the surface effect more obvious. As a limited case, when the pore radius is larger enough that k approaches zero, Eq. (9) will reduce to the classical solution without the surface effect as

$$M_{pl} = \frac{E(1-\xi)}{(1+v)[(1-2v)(1-\alpha)+(1-\alpha\xi)]\xi}. \tag{10}$$

Moreover, for the special case of neglecting the geometrical factor, $\alpha = 0$, Eq. (10) can be further reduced to the solution provided by Gor *et al.*[27]

In order to validate the proposed theoretical model of the pore-load modulus, the FEM simulations are performed to calculate to the adsorption-induced deformation of the ordered porous materials with triangular and square lattice. To simplify, here we just focus on the simplified model without the surface effect (Eq. (10)) in this case for the validation purpose. The boundary condition are set as the left and bottom surfaces are constrained in the x and y directions, respectively, while the right and top surface move freely (see Fig. 1(a)), to ensure the ordered porous plate can be freely expansion under the applied pressure at every pore. Numerical experiment shows that a model with the number of 15×17 unit cells for triangular (and 15×15 for square) lattice is sufficient to show the homogenized responses of porous materials. Moreover, mesh sensitivity study has been conducted to ensure the numerical convergence of the FEM models. The constituting solid skeleton is assumed to be silicon with Young's modulus $E = 130$GPa and Poisson's ratio $v = 0.28$.[27]

The FEM predicted porosity dependent pore-load modulus of the porous material, which are normalized by the Young's modulus of the solid matrix, are shown in Figs. 2(a) and 2(b) for the triangular and square lattice samples as red triangles, respectively. The corresponding theoretical predictions given by Eq. (10) with different geometrical arrangement factors are included as red solid lines for the purpose of comparison. For both the triangular and square lattice cases, one can

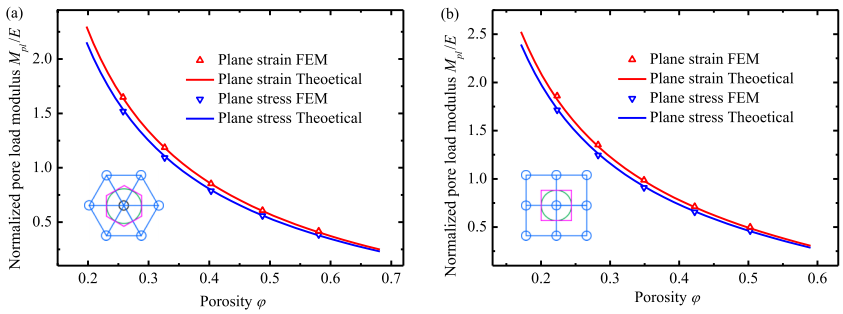

FIG. 2. Comparison of FEM and theoretical predictions of the normalized pore load modulus as a function of porosity: (a) the triangular lattice; (b) the square lattice.

see that our theoretical model agrees very well with the FEM results, with the maximum relative error being less than 5%. For the both lattice arrangements, the plane stress solutions are also plotted in the figures (shown as blue solid lines), with the corresponding FEM results included as blue inverted triangles for comparison. Again, excellent agreement between the FEM results and theoretical predictions is obtained. Eq. (10) can be adopted to estimate the pore-load modulus of the mesoporous material with macro-scale pores, where k approaches zero and the surface effect is negligible.

Now, let us revisit the adsorption-induced deformation of nanoporous materials, with the surface effect taken into account. A recent experiment is conducted by Gor *et al.*[27] They measured the adsorption-induced strain of a nanoporous silicon sample with a mean pore diameter of 8 nm and a volume porosity of 60%, and calculated the corresponding pore-load modulus from the measurement data. For the single-crystalline silicon used in their experiment, the bulk elastic constants are chosen as $E = 130\text{GPa}$ and $\upsilon = 0.28$, and the corresponding surface Lame constants, i.e., $\mu_S = -2.77\text{N/m}$ and $\lambda_S = -4.49\text{N/m}$, are adopted from the atomic simulation.[36]

Fig. 3 depicts the dependence of the normalized pore-load modulus on the porosity of the nanoporous sample. It clearly shows that the prediction given by the theoretical model incorporating surface effect (the blue solid line in Fig. 3 given by Eq. (9)) match the experimental data[27] (the black square) better than the classical theoretical prediction without surface effect (red solid line given by Eq. (10)). It is noted that some post-fabrication processes such as infiltration may result in negative surface elastic constants with greater absolute values. Under such circumstance, the actual surface Lame constants of the nanoporous sample used in the experiment may be less (with greater

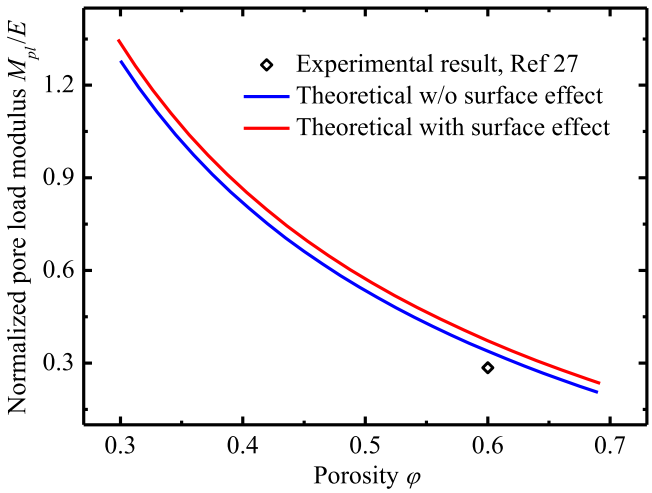

FIG. 3. Predictions of the pore load modulus by the theoretical model with/without surface effect.

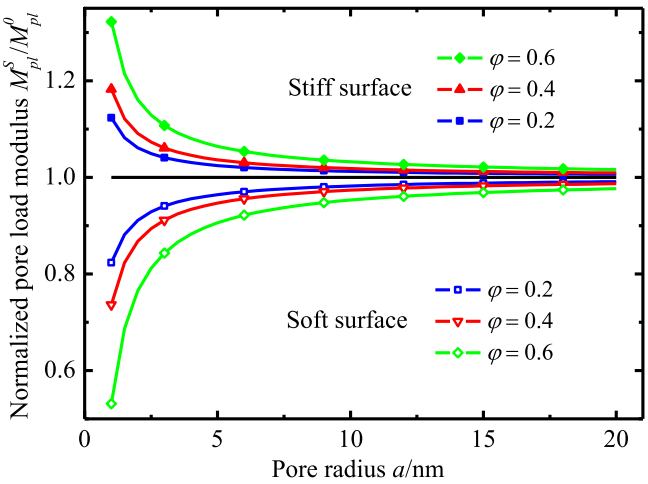

FIG. 4. Predictions for the size-dependent pore load modulus combining the different surface elastic constants.

absolute values) than the values used in our present predictions, leading to even lower predictions and approaching closer to the experimental results.

In order to further investigate the size-dependent effect of the pore-load modulus, the nanoporous materials with different pore radii and porosities are considered. Aluminum with Young's modulus $E = 90$GPa and Poisson's radio $\upsilon = 0.23$ is taken into consideration. Atomistic calculations indicate that a solid surface can be either elastically softer or stiffer than their bulk counterparts.[38] Thus, two typical sets of surface elastic constants for isotropic surfaces of aluminum are used[36]: $\mu_S = -6.22$ N/m and $\lambda_S = 3.49$N/m for the surface [1 0 0], $\mu_S = -0.38$N/m and $\lambda_S = 6.84$N/m for the surface [1 1 1]. It can be found the dimensionless parameter k is negative for the surface [1 0 0] and positive for the surface [1 1 1]. They can be called as "stiff" and "soft" surfaces, respectively.

The normalized pore-load moduli, predicted by using Eq. (9) for the two sets of surface properties, are plotted as a function of the pore radius in Fig. 4. Where the solid lines with open symbols and solid symbols denote stiff and soft surfaces, respectively, and three different porosities ($\varphi = 0.2$, 0.4 and 0.6) are considered with different colors. It can be found that the surface effects cause the pore-load modulus to decrease (increase) with reducing pore size for the soft (stiff) surface. Evidently, for both two surfaces, the surface effect on the pore-load modulus becomes more and more significant as the pore radius decreases less than 10 nm. Moreover, the surface effects are more prominent for a nanoporous sample with a higher porosity.

In conclusion, this work studied the influence of surface effect on the adsorption-induced deformation of the ordered nanoporous materials. An analytical solution for the pore-load modulus with surface effects was derived based on the single pore model of a pressurized thick-wall cylinder unit cell, and the surface elastic constants were adopted to describe the influence of surface energy. The proposed theoretical model are validated by comparing with FEM simulations for the limited case without surface effect and show great agreements, with the maximum relative error smaller than 5%. The model prediction clearly represents the experimentally observed soft pore-load modulus for nanoporous silicon. It also reveals that the surface effect plays an important role on the elastic response for nanoporous materials, and the pore-load modulus shows significant size-dependent characteristics. The present study warrants further qualitative studies in measuring the mechanical properties of nanoporous materials and in designing nanoporous material based sensors and actuators in various applications.

ACKNOWLEDGMENTS

The authors are grateful for the financial support of this work by the National Natural Science Foundation of China (No. 11472149) and the Tsinghua University Initiative Scientific Research Program (No. 2014z22074).

[1] M.E. Davis, Nature **417**, 813 (2002).
[2] G. Q. Lu and X. S. Zhao, *Nanoporous Materials - Science and Engineering* (Imperial College Press, London, 2004).
[3] M. J. Sailor, *Porous Silicon in Practice: Preparation, Characterization and Applications* (John Wiley & Sons, 2012).
[4] L. Canham, *Handbook of Porous Silicon* (Springer, 2015).
[5] G. Amato, C. Delerue, and H. J. VonBardeleben, *Structural and optical properties of porous silicon nanostructures* (CRC Press, 1998).
[6] D. Bellet, P. Lamagnere, A. Vincent, and Y. Brechet, J. Appl. Phys. **80**, 3772 (1996).
[7] C. Populaire, B. Remaki, V. Lysenko, D. Barbier, H. Artmann, and T. Pannek, Appl. Phys. Lett. **83**, 1370 (2003).
[8] S. Dourdain, D. T. Britton, H. Reichert, and A. Gibaud, Appl. Phys. Lett. **93**, 183108 (2008).
[9] L. H. Ma, Q. S. Yang, X. H. Yan, and Q. H. Qin, Mech. Mater. **73**, 58 (2014).
[10] J. C. Rasaiah, S. Garde, and G. Hummer, Annu. Rev. Phys. Chem. **59**, 713 (2008).
[11] G. Y. Gor and A. V. Neimark, Langmuir **26**, 13021 (2010).
[12] G. Y. Gor and A. V. Neimark, Langmuir **27**, 6926 (2011).
[13] F. T. Meehan, Proc. R. Soc. London A **115**, 199 (1927).
[14] D. H. Bangham and N. Fakhoury, Nature **122**, 681 (1928).
[15] O. K. Krasilnikova, B. P. Bering, V. V. Serpinskii, and M. M. Dubinin, Bull. Acad. Sci. USSR Div. Chem. Sci. **26**, 1099 (1977).
[16] G. Dolino, D. Bellet, and C. Faivre, Phys. Rev. B **54**, 17919 (1996).
[17] T. Herman, J. Day, and J. Beamish, Phys. Rev. B **73**, 094127 (2006).
[18] S. Dourdain, D. Britton, H. Reichert, and A. Gibaud, Appl. Phys. Lett. **93**, 183108 (2008).
[19] B. J. Melde, B. J. Johnson, and P. T. Charles, Sensors **8**, 5202 (2008).
[20] J. Biener, A. Wittstock, L. A. Zepeda-Ruiz, M. M. Biener, V. Zielasek, D. Kramer, R. N. Viswanath, J. Weissmuller, M. Baumer, and A. V. Hamza, Nature Mater. **8**, 47 (2009).
[21] J. Prass, D. Muter, P. Fratzl, and O. Paris, Appl. Phys. Lett. **95**, 083121 (2009).
[22] G. H. Findenegg, S. Jahnert, D. Muter, J. Prass, and O. Paris, Phys. Chem. Chem. Phys. **12**, 7211 (2010).
[23] N. Muroyama, A. Yoshimura, Y. Kubota, K. Miyasaka, T. Ohsuna, R. Ryoo, P. I. Ravikovitch, A. V. Neimark, M. Takata, and O. Terasaki, J. Phys. Chem. C **112**, 10803 (2008).
[24] A. Grosman, J. Puibasset, and E. Rolley, EPL **109**, 56002 (2015).
[25] G. Dolino, D. Bellet, and C. Faivre, Phys. Rev. B **54**, 17919 (1996).
[26] G. Gunther, J. Prass, O. Paris, and M. Schoen, Phys. Rev. Lett. **101**, 086104 (2008).
[27] G. Y. Gor, L. Bertinetti, N. Bernstein, T. Hofmann, P. Fratzl, and P. Huber, Appl. Phys. Lett. **106**, 261901 (2015).
[28] M. E. Gurtin and A. I. Murdoch, Int. J Solids Struct. **14**, 431 (1978).
[29] H. L. Duan, J. Wang, Z. P. Huang, and B. L. Karihaloo, J Mech. Phys. Solids **53**, 1574 (2005).
[30] D. Lu, Y. M. Xie, Q. Li, X. Huang, and S. Zhou, Appl. Phys. Lett. **105**, 101903 (2014).
[31] X. Q. Feng, R. Xia, X. Li, and B. Li, Appl. Phys. Lett. **94**, 011916 (2009).
[32] H. L. Duan, J. Wang, B. L. Karihaloo, and Z. P. Huang, Acta Mater. **54**, 2983 (2006).
[33] T. Chen, G. J. Dvorak, and C. C. Yu, Acta Mech. **188**, 39 (2007).
[34] S. G. Mogilevskaya, S. L. Crouch, A. La Grotta, and H. K. Stolarski, Compos. Sci. Technol. **70**, 427 (2010).
[35] P. Sharma, S. Ganti, and N. Bhate, Appl. Phys. Lett. **82**, 535 (2003).
[36] R. E. Miller and V. B. Shenoy, Nanotech. **11**, 139 (2000).
[37] S. Timoshenko and J. Goodier, *Theory of Elasticity*, 3rd ed. (McGrawHill, New York, 1970).
[38] L. G. Zhou and H. C. Huang, Appl. Phys. Lett. **84**, 1940 (2004).